Effect of transition metal oxide cocatalyst on the photocatalytic activity of Ag loaded $CaTiO_3$ for CO_2 reduction with water and water splitting

Tayyebeh Soltani,[a,*] Xing Zhu,[a] Akira Yamamomo,[a,b] Surya Pratap Singh,[a] Eri Fudo,[c] Atsuhiro Tanaka,[d,e] Hiroshi Kominami,[d] Hisao Yoshida[a,b,*]

[a] Graduate School of Human and Environmental Studies, Kyoto University, Kyoto 606-8501, Japan

[b] Elements Strategy Initiative for Catalysts and Batteries (ESICB), Kyoto University, Kyoto 615-8520, Japan

[c] Molecular and Material Engineering, Interdisciplinary Graduate School of Science and Engineering, Kindai University 3-4-1 Kowakae, Higashiosaka, Osaka 577-8502, Japan

[d] Department of Applied Chemistry, Faculty of Science and Engineering, Kindai University 3-4-1 Kowakae, Higashiosaka, Osaka 577-8502, Japan

[e] Precursory Research for Embryonic Science and Technology (PRESTO), Japan Science and Technology Agency (JST) 4-1-8 Honcho, Kawaguchi 332-0012, Japan

* Corresponding author: Tayyebeh Soltani, Tel: +81-75-753-6594, Fax: +81-75-753-2988

E-mail address: t.a_soltani@yahoo.com

* Corresponding author: Hisao Yoshida, Tel: +81-75-753-6594, Fax: +81-75-753-2988

E-mail address: yoshida.hisao.2a@kyoto-u.ac.jp

Abstract

Various dual cocatalysts consisting of Ag and transition metal oxide (TMO_x) were loaded on a $CaTiO_3$ (CTO) photocatalyst by different loading methods and examined for the photocatalytic CO_2 reduction with water as an electron donor. Compared to the results provided with the single Ag cocatalyst, the dual cocatalyst loaded CTO photocatalyst exhibited a similar or less CO evolution rate and higher H_2 production, meaning that these photocatalyst showed photocatalytic activity for both CO_2 reduction and water splitting. Dual cocatalysts of Ag and TMO_x loaded by a photodeposition gave higher CO production rate than those loaded by an impregnation method. The CTO photocatalysts with a single TMO_x cocatalyst showed higher activities in both the H_2 evolution and O_2 evolution test than the bare CTO and dual cocatalyst loaded CTO photocatalysts, indicating that the photocatalytic activity for water splitting is suppressed by the Ag cocatalyst but improved by the TMO_x.

Keywords: Photocatalytic conversion of CO_2; Water splitting; Transition metals; Dual cocatalyst; Calcium titanate

1. Introduction

In recent years, photocatalytic CO_2 conversion with water into useful compounds by using solar energy has been studied as an effective strategy in addressing global environmental issues [1]. This photocatalytic reaction uses H_2O as both a reductant (an electron donor) and a hydrogen source for the CO_2 reduction, and requires adequate band structure, i.e., both highly positive potential for H_2O oxidation and highly negative redox potential for CO_2 [2]. On the other hand, H_2 is also important for the sustainable society since this is a clean fuel and an important chemical resource.

Among several reductive products from CO_2 reduction, CO is a particularly important target product because it is a valuable chemical intermediate for further chemical syntheses and it can be easily separated from the aqueous reaction media to the gas phase [3]. At present, silver nanoparticles (Ag NPs) are widely considered to be one of the most efficient cocatalyst for heterogeneous semiconductor photocatalysts toward CO evolution in the photocatalytic CO_2 conversion with H_2O [4]. Recently, numerous photocatalysts such as $Ag/BaLa_4Ti_4O_{15}$ [4], Ag/Ga_2O_3 [5,6], $Ag/La_2Ti_2O_7$ [7], and $Ag/CaTiO_3$ [8,9] have been reported to exhibit high CO selectivity than that of H_2 by using Ag NPs as a cocatalyst.

In recent years, the design and synthesis of some dual cocatalysts by posing specified structures including core-shell type and two separate metal and oxide particles, such as Ag/Cu [10], Pt/Cu_2O [11], Ag/CrO_x[12], Cr/Rh [13] and Ag/MnO_x [14] are able to enhance CO_2 conversion activity or water splitting. The simultaneous introduction of two kinds of cocatalysts with two functional activity, a reduction cocatalyst and an oxidation cocatalyst, may result in many contact sites for improving both reduction and oxidation reactions, respectively. The arrangement of surface atom structure through crystal facet engineering and the appropriate set of conditions for the optimal preparation method could regulate surface free energy, electronic band structure,

charge transfer and separation, and surface redox site [15], thus would bring sustainable solutions for the low catalytic activity of many photocatalysts and the materials with unprecedented photocatalytic activities will be possible [16].

In our previous studies, we successfully improved the photocatalytic activity of $CaTiO_3$ photocatalyst (CTO) for CO_2 reduction to CO and O_2 by using Ag NPs as a cocatalyst, where the product selectivity (S_{CO}) to CO among possible reductive products was as high as 96% [8,9]. In the present study, we prepared CTO by a flux method, which tends to give fine crystals, and loaded both Ag NPs and various transition metal oxides (TMO_x) as dual cocatalysts by some methods, and examined their photocatalytic activities in the photocatalytic CO_2 reduction with water, where H_2 can be formed via water splitting as a competitive reaction.

2. Experimental section

2.1. Preparation of samples

The CTO samples used here was prepared by a flux method in the same manner as our previous work [9]. Starting materials, $CaCO_3$ (Kojundo, 99.99%), rutile TiO_2 (Kojundo, 99.9 %) as solutes and NaCl (Kishida 99.5%) as a flux were weighted and mixed physically in a mortar, where the molar ratio of $CaCO_3$ to TiO_2 was 1.05:1, and that of CTO to NaCl was 1:1. The mixture was put into an alumina crucible, which was loosely covered by a lid, heated in an electric furnace at a rate of 200 K h^{-1} up to 1473 K, held at this temperature for 10 h, and then slowly cooled at a rate of 100 K h^{-1} to 773 K, followed by being naturally cooled to room temperature. The obtained powder was thoroughly washed with hot water (353 K, 500 mL) for 15 minutes and filtrated, and this washing step was repeated 3 times to completely remove any residual salt, then dried at 373 K for 24 h to obtain the CTO sample.

Two methods, a photodeposition method (PD) and an impregnation method (IMP), and their combinations were examined for loading of Ag and TMO_x (TMO_x=NiO_x, CoO_x, FeO_x) dual cocatalysts on the CTO sample. The loading amounts in the present study were desired to be 2.0 and 0.5 wt% for Ag and TMO_x species, respectively, for all the samples.

In the simultaneous PD method, 1 g of the CTO sample was dispersed in 360 mL of pure water containing both $AgNO_3$ and a required precursor such as $Ni(NO_3)_2.6H_2O$, $Co(NO_3)_2.6H_2O$ and $Fe(NO_3)_2.6H_2O$, in an inner-irradiation-type reaction vessel, and a bubbling flow of Ar gas was used to exclude the air for 1 h before photoirradiation. Then the suspension was photoirradiated from the center of the vessel by a 100 W high-pressure Hg lamp located with a bubbling flow of Ar gas for 2.5 h. Then, the resulting suspension was filtered and dried in air at 373 K for 24 h. These samples were referred to as Ag(PD)-TMO_x(PD)/CTO samples.

Additional two samples were prepared by a two-step PD method, in which Ag and NiO_x species were consecutively photodeposited one by one on the CTO photocatalyst: Ag species was first photodeposited on the CTO sample, followed by the photodeposition of NiO_x species to give the NiO_x(PD)/Ag(PD)/CTO sample, while the Ag(PD)/NiO_x(PD)/CTO sample was prepared in the reverse order.5

In the simultaneous IMP method, the CTO sample was soaked in a solution (50 ml) containing the two precursors for Ag and TMO_x and continuously stirred in a water bath at 120 rpm at 353 K to completely evaporate whole of water. Then, the resulting samples were dried in air at 373 K for 24 h, and calcined at 723 K for 1 h in the furnace. The samples were denoted as Ag(IMP)-TMO_x(IMP)/CTO samples.

In a combination of the IMP and PD methods, a TMO_x species was first loaded by the IMP method, followed by loading Ag with the PD method, providing the Ag(PD)/TMO_x(IMP)/CTO samples. The NiO_x(IMP)/Ag(PD)/CTO sample was prepared in the inversed order.

The single Ag cocatalyst sample and the single TMO_x cocatalyst samples were also prepared such as the Ag(PD)/CTO, TMO_x(PD)/CTO, and TMO_x(IMP)/CTO samples.

2.2. Characterization

The X-ray diffraction (XRD) patterns of all samples were recoded with a Lab X XRD-6000 (Shimazu). Morphologies of the samples were obtained by scanning electron microscopy (SEM) with a JSM-890 (JEOL). Transmission electron microscopy (TEM) images were acquired out with energy dispersive X-ray analysis (EDX) by a JEOL JEM-2100F at 200 kV in the Joint Research Centre of Kindai University. Ag K-edge X-ray absorption fine structures (XAFS) were recorded at BL01B1 of SPring-8 (Hyogo, Japan) in a transmission mode with a Si(311) double crystal monochromator. The actual loaded amounts of cocatalysts was evaluated by XRF with an EDX-8000 (Shimadzu) according to each calibration curve that was experimentally obtained from a series of reference samples prepared by the impregnation method. The diffuse reflectance (DR) UV–visible spectra were measured using a V-670 (JASCO) equipped with an integrating sphere covered with $BaSO_4$, which was used as the reference.

2.3. Photocatalytic reaction test

Photocatalytic activity test for CO_2 reduction by H_2O was carried out using a flow system with an inner-irradiation-type reaction vessel at ambient pressure [3]. The photocatalyst (0.3 g) were dispersed in ion-exchanged water (350 mL) containing 0.5 M $NaHCO_3$, and then suspended with magnetically stirring in a bubbling flow of gaseous CO_2

at a flow rate of 30 mL min^{-1} without radiation for 1 h. The photocatalytic reaction was performed at reaction temperature of 290 K by using a 100 W high-pressure mercury lamp with 44 mW cm^{-2} measured at 254 ± 10 nm in wavelength. The amounts of evolved CO, H_2 and O_2 were detected by using an on-line gas chromatograph (Shimadzu, GC-8A, TCD, Shincarbon ST column, argon carrier). The CO, H_2 and O_2 were generated as the main product under photoirradiation, where CO was the main reductive product from CO_2 and H_2 was produced by water splitting as a competitive reaction [17]. The selectivity toward CO evolution among the reductive products, S_{CO}, and the ratio of the consumed electrons and holes, $R(e^-/h^+)$, were calculated using the formulae shown below [18],

$$S_{CO}(\%) = R_{CO} \times 100/(R_{CO} + R_{H_2})$$

$$R(e^-/h^+) = (R_{CO} + R_{H_2})/2R_{O_2}$$

where R_{CO}, R_{H2}, and R_{O2} describe the production rate of CO, H_2, and O_2, respectively.

In the H_2 evolution tests, we added methanol as an electron donor (a reductant) to make the reductive reaction to be the rate determining step, while in the O_2 evolution test $NaIO_3$ (10 mM) was added as an electron acceptor (an oxidant) to make the oxidative reaction to be the rate determining step.

3. Results and discussion

3.1. Characterization of the sample

The actual loaded amounts of cocatalysts was evaluated by XRF and listed in Table S1and Table S2. Although the desired loading amounts in both the single and dual cocatalyst samples were 2.0 and 0.5 wt.% for Ag and TMO_x species, respectively, the amount of TMO_x cocatalyst loaded by the PD method was actually less than the desired value. In the PD method, although Ag^+

can be easily reduced to form metallic Ag, it is considered that photocatalytic reduction and oxidation of transition metal cations would be more difficult [19].

The XRD patterns of the CTO, Ag(PD)/CTO and Ag(PD)-TMO_x(PD)/CTO samples evidenced the formation and conservation of the $CaTiO_3$ perovskite crystal, and new peak at about 38.2° assignable to Ag metal was observed after loading Ag species (Fig.1A). However, no diffraction lines corresponding to transition metal oxide was not obvious in whole samples. In these samples, the content of the transition metal oxide was very low as mentioned above, which would be lower than the detection limit in the present conditions and thus no diffraction from them was observed.

Ag K-edge X-ray absorption near edge structure (XANES) of the Ag(PD)/CTO sample was similar to that of Ag foil, meaning that these Ag NPs were metallic state in this sample (Fig.1Bb). Although XANES of other samples were not measured in this study, it is reported in our previous study that the Ag species in a silver–manganese dual cocatalyst on potassium hexatitanate photocatalyst loaded by the same photodeposition method was metallic state according to Ag K-edge XANES [3,19]. This means that the coexistence of the second cocatalyst would not significantly change the chemical state of Ag NPs in the dual cocatalyst system, suggesting that the Ag species would be metallic also in the present samples. This is supported by the XRD (Fig. 1A) as mentioned and the DR UV-visible spectra (Fig. 4 and 6) as mentioned later.

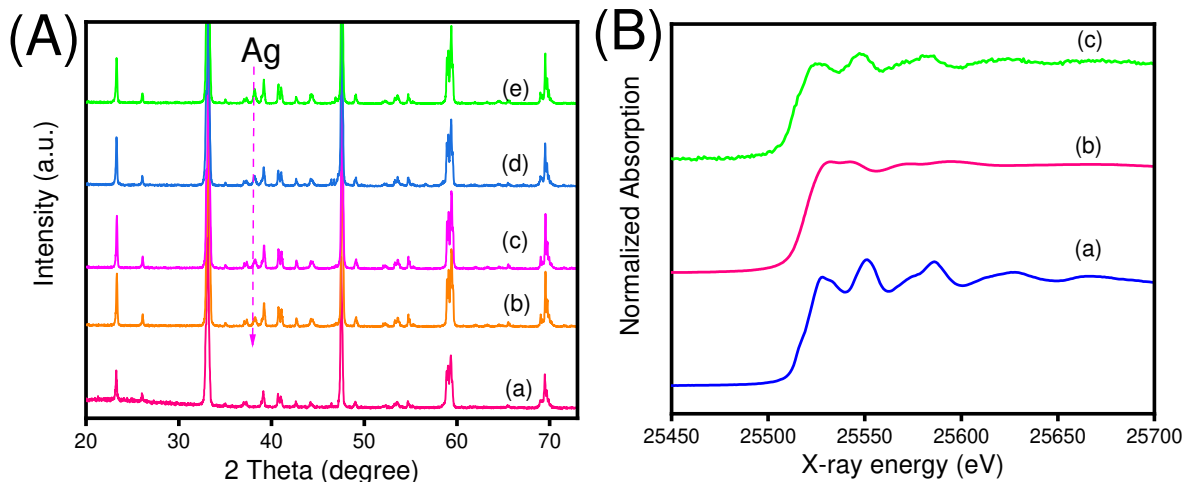

Fig. 1. [A] XRD spectra of the samples; (a) bare CTO, (b) Ag(PD)/CTO, (c) Ag(PD)-NiO_x(PD)/CTO, (d) Ag(PD)-CoO_x(PD)/CTO, and (e) Ag(PD)-FeO_x(PD)/CTO. [B] Ag K-edge XANES of the samples; (a) Ag foil, (b) Ag_2O, and (c) Ag(PD)/CTO.

The SEM image of the CTO sample shown in Fig. 2a reveals that these particles consisted of the polyhedral crystal shape covered with many facets. On the Ag(PD)/CTO sample, Ag NPs were successfully distributed on the dominant facets (Fig. 2b). The SEM image of the as-synthesized Ag(PD)-NiO_x(PD)/CTO sample show the presence of additional particles on the CTO crystals, although it is difficult to distinguish the Ag and NiO_x species on these samples (Fig. 2c). TEM images also confirm that no NPs were found on the surface of the bare CTO sample (Fig. 2d), and the spherical Ag NPs sized in the range of 30–40 nm were loaded on the CTO surface (Fig. 2, e and f).

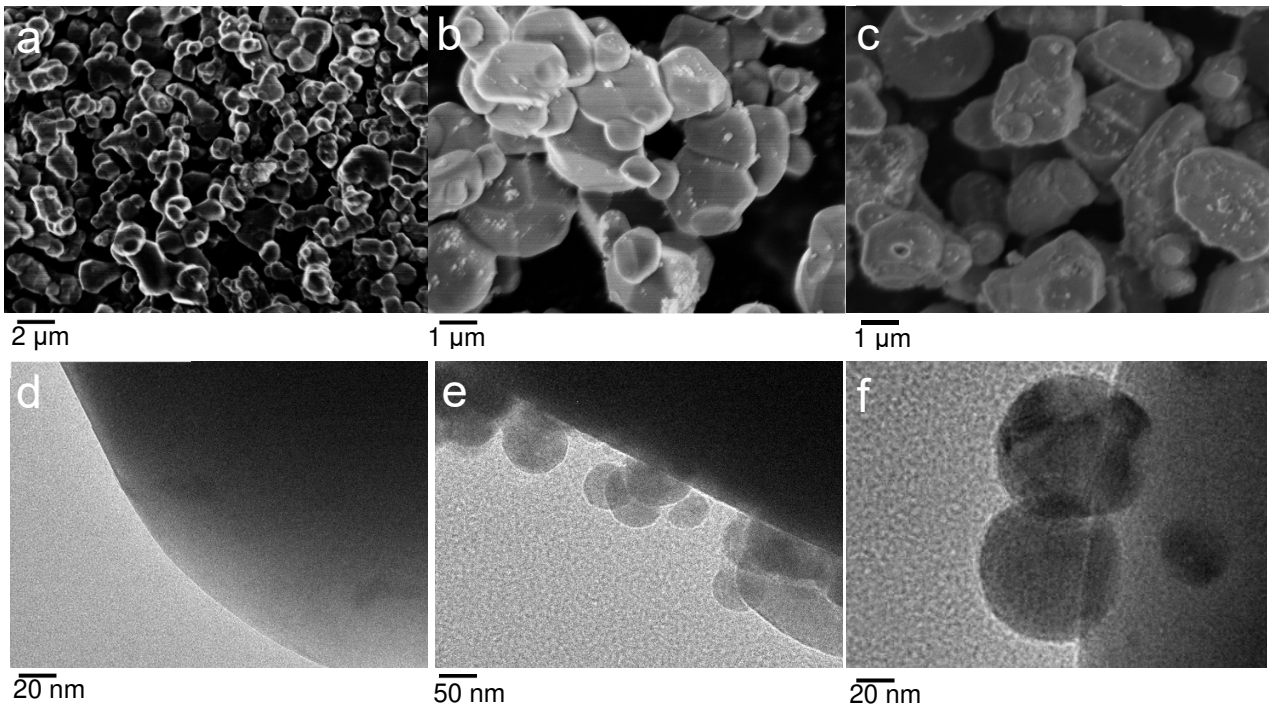

Fig. 2. (a-c) SEM and (d-f) TEM images of the prepared samples; (a,d) CTO, (b, e,f) Ag(PD)/CTO, and (c) Ag(PD)-NiO_x(PD)/CTO.

3.2. CO_2 reduction results

3.2.1. Ag-TMO_x/ CTO photocatalyst

Photocatalytic activity tests in the photocatalytic CO_2 reduction with water were carried for the various samples, which were prepared with the PD method and the combination of IMP and PD methods, and results are as shown in Fig. 3. The observed products were CO, H_2, and O_2, where CO was the reductive product from CO_2 in the aid of water, and H_2 was produced via water splitting as a competitive reaction (Eq. 1 and 2), respectively, [8,20], and water was oxidized to O_2 (Eq. 3) that is the common product of the CO_2 reduction and water splitting [12,19,21].

$$CO_2(g) + 2H^+ + 2e^- \rightarrow CO(g) + H_2O(l) \qquad E^{\ominus}(CO_2/CO) = -0.106 \text{ V vs. RHE} \qquad (1)$$

$$2H^+ + 2e^- \rightarrow H_2(g) \qquad E^{\ominus}(H^+/H_2) = 0\ \text{V vs. RHE} \qquad (2)$$

$$2\,H_2O\,(l) + 4\,h^+ \rightarrow O_2(g) + 4H^+ \qquad E^{\ominus}(O_2/H_2O) = +1.23\ \text{V vs. RHE} \qquad (3)$$

As shown in Fig. 3a**,** the bare CTO sample without any cocatalyst mainly promoted water splitting with the formation of H_2 and O_2. The Ag(PD)/CTO photocatalyst exhibited high CO formation rate (7.31 μmol h^{-1}) and high selectivity (S_{CO} = 96 %) by suppressing H_2 formation via water splitting (Fig. 3b). The ratio of the number of reacted electrons to that of holes was almost unity, $R(e^-/h^+)$=1.06, suggesting that both the reductive and oxidative products were observed in a stoichiometric ratio. Compared with the Ag(PD)/CTO sample, the dual cocatalyst loaded Ag(PD)-TMO_x(PD)/CTO samples prepared by the simultaneous PD method exhibited comparable or less CO production rates and higher H_2 formation rates (Fig. 3c-e). The selectivity of the reductive products depended on the composition of the cocatalysts. Among them, the Ag(PD)-NiOx(PD)/CTO sample showed the moderately high activities for both CO and H_2 productions (Fig. 3c), where the CO selectivity S_{CO} was 58%. In contrast, the Ag(PD)-CoO_x(PD)/CTO and Ag(PD)-FeO_x(PD)/CTO samples gave lower S_{CO} (Fig. 3d and e), and the latter sample dominantly produced H_2 with very low S_{CO} (7.5%).

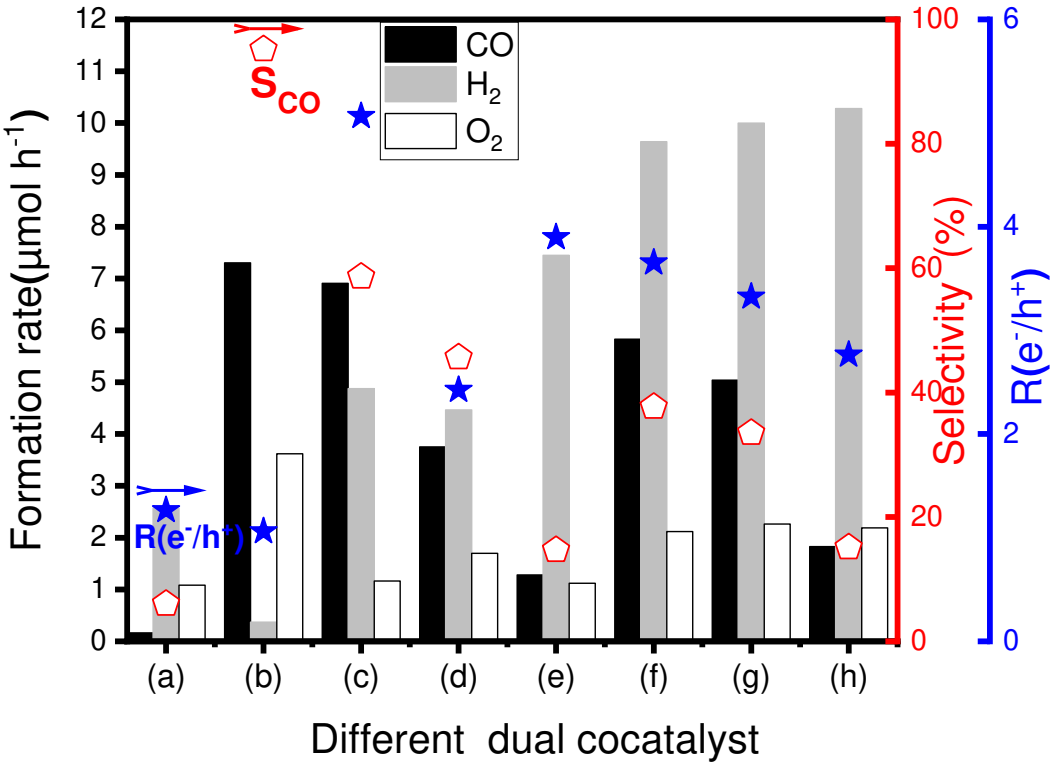

Fig. 3. Formation rates of CO, H_2, and O_2, and the CO selectivity, S_{CO}, and the electron and hole ratio consumed for the gaseous product formation, $R(e^-/h^+)$, in the photocatalytic reaction test for CO_2 conversion in the aqueous solution with the photocatalyst samples; (a) CTO, (b) Ag(PD)/CTO, (c) Ag(PD)-NiO_x(PD)/CTO, (d) Ag(PD)-CoO_x(PD)/CTO (e) Ag(PD)-FeO_x(PD)/CTO, (f) Ag(PD)/NiO_x(IMP)/CTO, (g) Ag(PD)/CoO_x(IMP)/CTO, and (h) Ag(PD)/FeO_x(IMP)/CTO. The data were taken after the photoirradiation for 4.5 h.

The samples prepared by the combination of the IMP and PD methods, Ag(PD)/TMO_x(IMP)/CTO samples, exhibited higher H_2 formation rate than the Ag(PD)-TMOx(PD)/CTO samples (Fig. 3, f–h). To confirm the property of the transition metal species, the TMO_x single cocatalyst loaded samples, TMO_x(PD)/CTO and TMO_x(IMP)/CTO, were also prepared and examined in the photocatalytic reaction test (Fig. S1). These photocatalysts could not produce CO at all, indicating the Ag cocatalyst is intrinsically required for CO_2 reduction to CO and these transition metal cannot function as the cocatalyst for CO formation from CO_2. Among

these single cocatalyst loaded photocatalysts, the samples prepared by the IMP method (Fig. S1, f–h) showed higher activity for water splitting than the samples prepared by the PD method (Fig. S1, c–e), which might be due to the larger loading amount as shown in Table S1. These properties of the TMO_x single cocatalyst loaded photocatalyst (Fig. S1) are somewhat similar to the Ag(PD)-TMO_x dual cocatalyst loaded photocatalyst (Fig. 3) except for the CO formation. Thus, the TMO_x species in the dual cocatalyst would contribute to the water splining only. In addition, it is found that the TMO_x species in the dual cocatalyst loaded samples (Fig. 3) exhibited higher activities than those in the TMO_x(IMP)/CTO samples (Fig. S1), suggesting that TMOx species coexisting with Ag NPs prepared by the PD method have high activity for water splitting. The impregnation method would certainly form the transition metal oxide species while the following photoirradiation might partially form reduced state of the TMO_x species. In the DR UV-visible spectra (Fig. 4), the Ag(PD)/TMO_x(IMP)/CTO samples exhibited the localized surface plasmon resonance (LSPR) bands of Ag NPs at the position around 380–530 nm in wavelength, which is similar to the Ag(PD)/CTO sample, confirming that Ag NPs were present in these samples, and they would almost be in a similar state, regardless of the presence of the metal oxide species (Fig. 4). This propose that the Ag NPs are independently present with the TMO_x species.

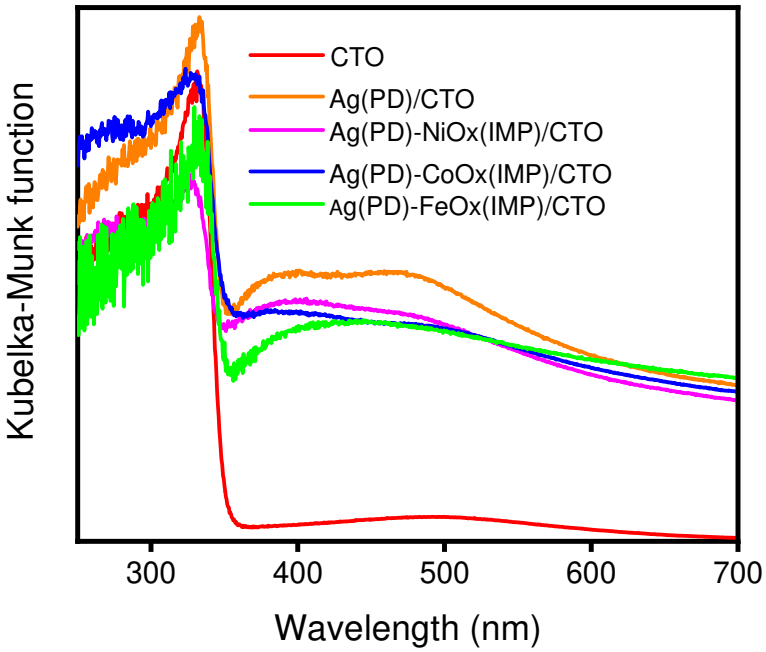

Fig. 4. DR UV–Visible spectra of the samples; bare CTO, Ag(PD)/CTO, Ag(PD)/NiO_x(IMP)/CTO, Ag(PD)/CoO_x(IMP)/CTO, and Ag(PD)/FeO_x(IMP)/CTO.

In contrast to reduction products (H_2 and CO), the O_2 evolution was insufficient in induction time period (4.5 h light illumination) for all the Ag-TMO_x dual cocatalyst loaded CTO photocatalysts. One may think that one possible reason is the difficulty of water oxidation due to the high overpotential of O_2 evolution, which probably originate from the formation of deep trapping and stabilization of positive charge by the surface sites [22,23]. However, if holes are not consumed, the formation of reductive products (CO and H_2) should be significantly prohibited. And it was the fact that reductive products were observed. These facts suggest that a certain oxidative reaction by holes would take place on the surface of catalyst. Thus, other possibilities should be considered for this phenomenon. One is that produced O_2 may be dissolved in the aqueous $NaHCO_3$ solution, or adsorbed on the catalyst surface [20] and another is that some

competitive side reactions may occur [20,24]. As mentioned later, the O_2 evolution increased with time on the Ag(PD)-TMO_x(PD)/CTO sample (Fig. 5B), suggesting that the produced O_2 might be dissolved in the solution, adsorbed on the catalyst surface, or stored as different intermediates such as H_2O_2. As for this point, further investigations are required.

3.2.2. Ag-NiOx/CTO photocatalysts prepared by different loading method

Some Ag-NiOx/CTO samples were prepared by different preparation methods and examined for the photocatalytic activity tests (Fig. 5A). The Ag(PD)-NiO_x(PD)/CTO and Ag(PD)/NiO_x(IMP)/CTO samples provided moderately high CO formation as mentioned above (Fig. 5A, a and b and also Fig. 3, c and f) although the latter showed higher activity for H_2 formation. These samples had the photodeposited Ag NPs showing the LSPR bands (Fig. 6) although the state of the NiO_x species would be different due to the difference of the preparation method. Thus, the photocatalytic activity of Ag NPs for reduction of CO_2 to CO was not so related to the state of the NiO_x species. The Ag(IMP)-NiOX(IMP)/CTO sample showed low photocatalytic activity for both CO_2 reduction and water splitting (Fig. 5Ac). In this sample prepared by the simultaneous IMP method, both Ag and Ni species were oxidized, and they possibly would be mixed together to have interaction, resulting less activity. The NiO_x(IMP)/Ag(PD)/CTO sample (Fig. 5Ad) exhibited high H_2 formation rate and much less CO formation rate, and did not exhibit clear LSPR bands due to Ag NPs and the broad band would be assignable to the NiOx species (Fig. 6). These results clarified that the independently existing NiO_x species can act as cocatalyst for water splitting and the Ag species oxidized by the calcination at the second step cannot function as cocatalyst for CO_2 reduction to form CO.

Additional two samples, NiO_x(PD)/Ag(PD)/CTO and Ag(PD)/NiO_x(PD)/CTO, were prepared by a consecutive two-step PD method and examined for the photocatalytic reaction test (Fig. S2). These samples also exhibited highly enhanced photocatalytic activities, which were similar to that of the Ag(PD)-NiO_x(PD)/CTO sample prepared by the simultaneous PD method. This result indicates that the effect of photodepositted NiO_x species on photocatalytic activity was not related to the order of the photodeposition, which is in accordance with our previous results [19].

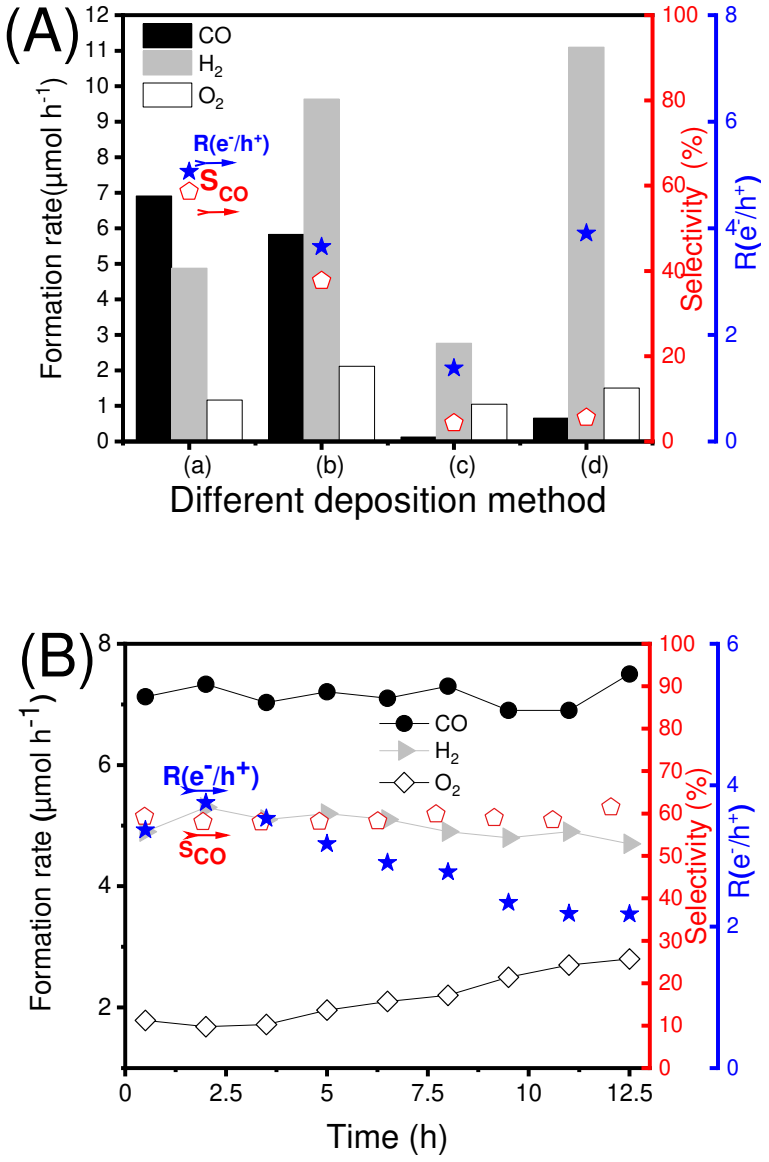

Fig. 5. [A] Formation rates of CO, H_2, and O_2, the CO selectivity in the reductive products (S_{CO}), and the electron and hole ratio consumed for the gaseous product formation $R(e^-/h^+)$, in the photocatalytic reaction test for CO_2 conversion in the aqueous solution over the photocatalyst samples; (a) Ag(PD)-NiO_x(PD)/CTO, (b) Ag(PD)/NiO_x(IMP)/CTO, (c) Ag(IMP)-NiO_X(IMP)/CTO, and (d) NiO_x(IMP)/Ag(PD)/CTO. The data were taken after the photoirradiation for 4.5 h. [B] Time course of the production rates in the gas phase, S_{CO}, and $R(e^-/h^+)$ in the photocatalytic reaction test for CO_2 conversion in the aqueous solution with the Ag(PD)-NiO_x(PD)/CTO sample.

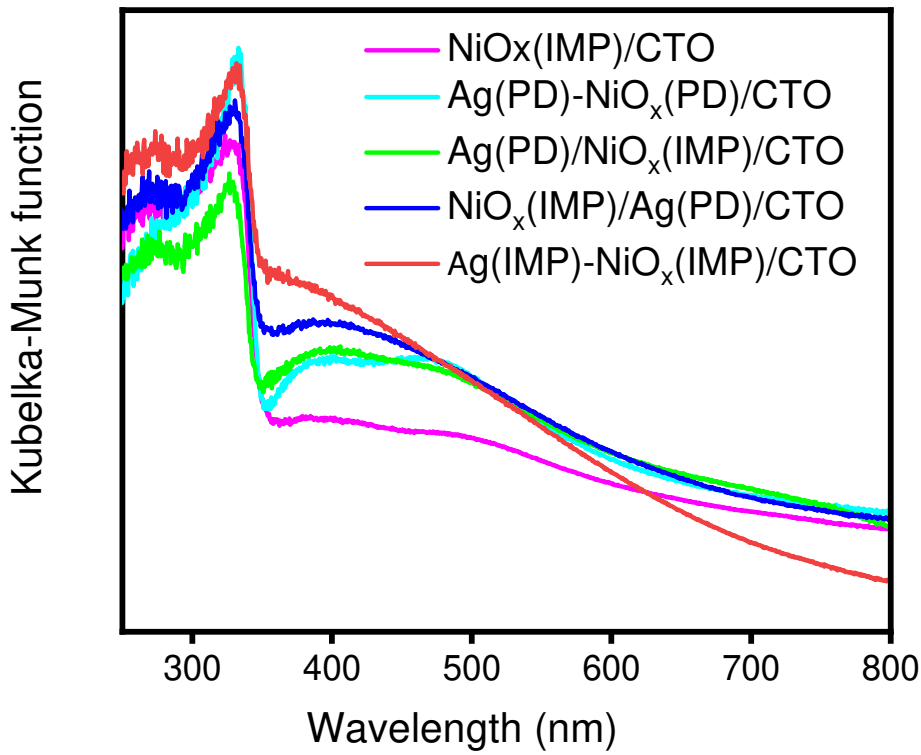

Fig. 6. DR UV–Visible spectra of the samples; NiO_x(IMP)/CTO, Ag(PD)-NiO_x(PD)/CTO, Ag(PD)/NiO_x(IMP)/CTO, NiO_x(IMP)/Ag(PD)/CTO, and Ag(IMP)-NiO_x(IMP)/CTO.

Based on these observations, we can conclude that the metallic Ag NPs prepared by the PD method can function as selective cocatalyst for CO formation, while the TMO_x cocatalyst can contribute to water splitting more effectively when they are prepared by impregnation method and present independently with Ag species.

The O_2 evolution recorded in the initial period (4.5 h) was insufficient for these samples, resulting in the very high R(e^-/h^+) values. However, the production rate of O_2 over the Ag(PD)-NiO_x(PD)/CTO photocatalyst gradually increased with irradiation time and thus more stoichiometric production of reductive and oxidative products was continuously observed after irradiation of 12.5 h for (Fig. 5b).

3.3. H_2 evolution test

To figure out the role of NiO_x, CoO_x and FeO_x in H_2 production, H_2 evolution test for whole of single and dual cocatalyst loaded on CTO was also performed in the presence of methanol as an electron donor, and results are shown in Fig. 7A. The results obtained from H_2 evolution test shows that high H_2 yields of 467 μmol, 408 μmol and 351 μmol for 7.5 h were obtained with a single FeO_x, CoO_x and NiO_x cocatalyst, respectively, which was 1.22-fold, 1.14-fold and 1.32-fold higher than those with the dual cocatalyst loaded photocatalysts: Ag(PD)/FeO_x(IMP)/CTO (381 μmol), Ag(PD)/CoO_x(IMP)/CTO (358 μmol), and Ag(PD)/NiO_x(IMP)/CTO (265 μmol). The bare CTO and Ag(PD)/CTO showed the H_2 formation of 161 and 96 μmol, respectively, for 7.5 h, which were lower than that those with TMO_x. This means that the Ag NPs is effective cocatalyst not for water splitting but for CO_2 reduction [8]. The higher H_2 evolution activity with a single TMO_x co-catalyst than the Ag-TMO_x dual cocatalyst, proposed that the coexist Ag NPs inhibited the H_2 production[25].

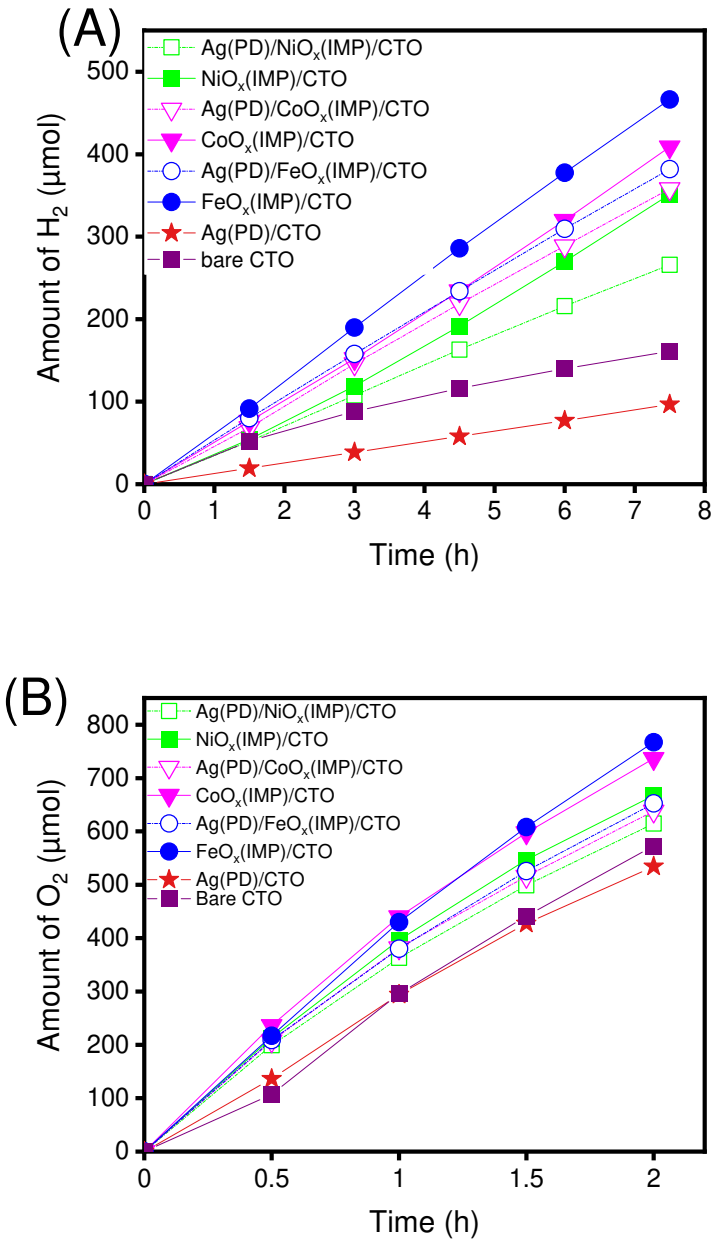

Fig. 7. [A] Time course of H_2 evolution from an aqueous methanol solution with different single and dual cocatalyst loaded CTO photocatalyst samples; Ag(PD)/NiO_x(IMP)/CTO, NiO_x(IMP)/CTO, Ag(PD)/CoO_x(IMP)/CTO, CoO_x (IMP)/CTO, Ag(PD)/FeO_x(IMP)/CTO, FeO_x(IMP)/CTO, Ag(PD)/CTO and bare CTO , where methanol was used as an electron donor. [B]Time course of O_2 evolution test from an aqueous solution of $NaIO_3$ with the photocatalyst samples; Ag(PD)/NiO_x(IMP)/CTO, NiO_x(IMP)/CTO, Ag(PD)/CoO_x(IMP)/CTO, CoO_x (IMP)/CTO, Ag(PD)/FeO_x(IMP)/CTO, FeO_x(IMP)/CTO, Ag(PD)/CTO and bare CTO, where $NaIO_3$ was used as electron acceptor.

3.4. Oxygen evolution test

To clarify the role of the TMO_x species in O_2 production, oxygen evolution test was also performed for whole of single and dual cocatalyst loaded on CTO and the results are shown in Fig. 7B. The bare CTO were active towards water oxidation, with the corresponding O_2 evolution amount reaching 573 μmol after 2 h of illumination, suggesting that surface of bare CTO provides suitable sites for water oxidation. In the case of the Ag(PD)/CTO, no apparent increase in O_2 evolution amount was observed as compared to bare CTO, meaning that Ag cocatalyst can be considered as a promising candidate for the reduction of CO_2 to CO, and only hole from CTO photocatalysts were active towards water oxidation. The O_2 evolution performance of the sample with a single FeO_x, CoO_x and NiO_x cocatalyst, respectively, was 767, 736 and 667 μmol, which was higher than those with the dual cocatalyst loaded photocatalysts: Ag (PD)/FeO_x(IMP)/CTO (652 μmol), Ag(PD)/CoO_x(IMP)/CTO (637 μmol), and Ag(PD)/NiO_x(IMP)/CTO (614 μmol). This means that the addition of Ag NPs seems to decrease O_2 evolution formation. These results are consistent with the previous H_2 evolution results with the single FeO_x, CoO_x and NiO_x cocatalyst, where active sites for H_2 evolution are reduced by Ag species (Fig. 7A). Moreover, the O_2 evolution performance of the samples with a single TMO_x co-catalyst or the Ag-TMO_x dual cocatalyst was also higher than that with the bare CTO (573 μmol) or Ag/CTO (534 μmol) photocatalyst. Enhanced O_2 evolution performance in the presence of TMO_x species can be ascribed to the effective role of TMO_x as an oxide-based cocatalysts in facilitating the charge carrier separation and/or acting as water oxidation sites, in accordance with other literature reports [26,27]. These results represented that the sample with a single TMO_x cocatalyst showed higher activities in both the H_2 evolution and O_2 evolution test

with each sacrifice reagent. Moreover, the coexistence of Ag NPs species would diminish the active sites for both H_2 and O_2 evolution.

3.5. Proposed mechanism

Here, we propose a mechanism for the photocatalytic CO_2 reduction into CO on Ag-TMO_x dual cocatalyst loaded CTO photocatalyst. In the case of the photocatalytic CO_2 reduction with water on the Ag/CTO photocatalyst, the Ag cocatalyst can receive the photoexcited electrons from the conduction band of the CTO and function as a reduction sites predominantly for production of CO as shown in Eq. (1) [8] (Scheme 1a). On the Ag-TMO_x/CTO photocatalyst, the coexistence of the Ag and TMO_x species in the dual cocatalyst on the CTO photocatalyst was beneficial for both CO_2 reduction and waters splitting with the formation of a significant amount of H_2 as a second reductive product via water splitting, where the two reactions competitively proceeded. However, the actual role of these transition metal oxide species as cocatalysts for overall water splitting is still under debate. It has been proposed that transition metal can be reformulated as oxidized species, TMO_x, on the CTO photocatalyst, in which TMO_x actually functions as the proton reduction sites to produce H_2 and as the water oxidation sites to produce O_2 (Scheme 1b), respectively. Zhang et al. studied the critical role of NiO_x cocatalyst for overall water splitting using $NaTaO_3$ as photocatalyst [28]. They found that although NiO was solely deposited on the surface of $NaTaO_3$, the existence of both metallic Ni and NiO were observed during photocatalytic reaction, and the actual roles of metallic Ni as an electron trap (the catalytic sites for proton reduction) and NiO as a hole trap (the catalytic sites for water oxidation) were confirmed by X-ray photoelectron spectroscopy and synchrotron X-ray absorption spectroscopy. However, the main role of TMO_x as the surface reaction sites in water splitting as well as the facet charge separation are not well clarified and need to be further addressed in our next study.

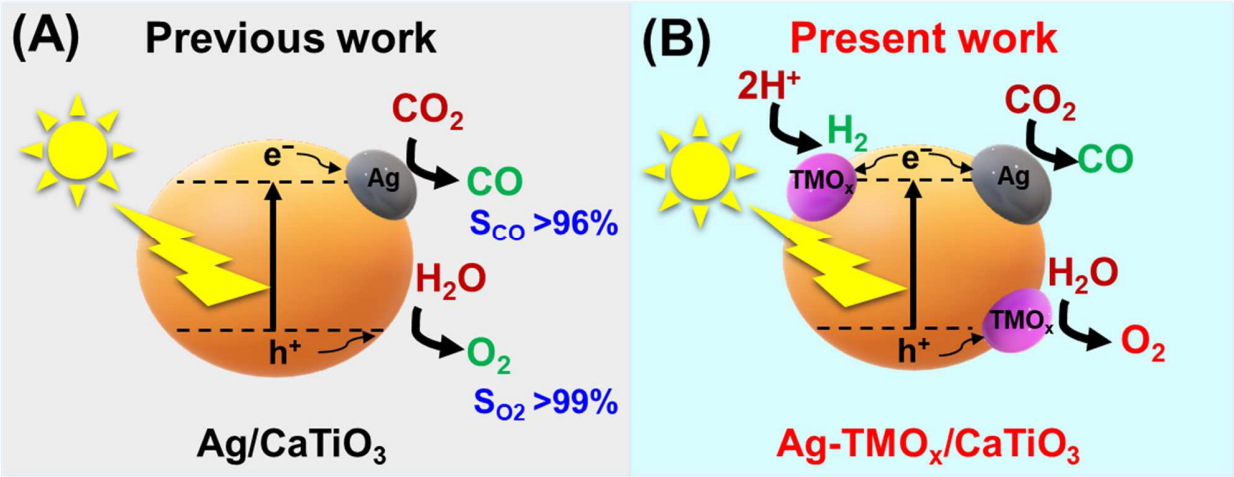

Scheme 1. Proposed mechanisms for the photocatalytic CO_2 reduction with water and water splitting over [A] the Ag single cocatalyst loaded CTO photocatalyst and [B] the Ag-TMO_x dual cocatalyst loaded on CTO photocatalyst.

4. Conclusion

In this study, the effects of the Ag-TMO_x dual cocatalyst (M=Fe, Co, Ni) and the loading method on the activity of the CTO photocatalyst for CO_2 conversion to CO and O_2 and water splitting to H_2 and O_2 were investigated and the following matters were clarified.

1) Compared to the single Ag co-catalyst, the Ag–TMO_x dual cocatalyst provided a comparable or less activity for CO evolution and a higher activity for H_2 evolution.
2) The photocatalytic activity depended on the loading method. The photodeposition method gave higher activity for CO formation and the impregnation method gave higher activity for H_2 formation.
3) A TMO_x cocatalyst can improve the activity of the CTO photocatalyst for water splitting to form H_2 and O_2 while the Ag cocatalyst can improve the activity for not the water splitting but CO_2 reduction.

Declaration of Competing Interest

The authors declare no competing financial interest.

Acknowledgements

The XANES measurements were performed at the BL01B1 of SPring-8 with the approval of the Japan Synchrotron Radiation Research Institute (JASRI) (Proposal No. 2015B1275 and 2019B1515). This work was financially supported by a Grant-in-Aid for JSPS Fellows (19F19351) from the Japan Society for the Promotion of Science (JSPS), the Masuya Memorial Basic Research Foundation, ISHIZUE 2020 of Kyoto University Research Development Program, the joint research program of the Artificial Photosynthesis, Osaka City University, and the Program for Elements Strategy Initiative for Catalysts and Batteries (ESICB, JPMXP0112101003), commissioned by the MEXT of Japan. T.S. would like to thank JSPS for providing Invitational Fellowships for Research in Japan.

References

[1] C. Vezzoli, F. Ceschin, L. Osanjo, M.K. M'Rithaa, R. Moalosi, V. Nakazibwe, J.C. Diehl, Energy and sustainable development BT - Designing sustainable energy for all: sustainable product-service system design applied to distributed renewable energy, in: C. Vezzoli, F. Ceschin, L. Osanjo, M.K. M'Rithaa, R. Moalosi, V. Nakazibwe, J.C. Diehl (Eds.), Springer International Publishing, Cham, 2018: pp. 3–22.

[2] J. Qiao, Y. Liu, F. Hong, J. Zhang, A review of catalysts for the electroreduction of carbon dioxide to produce low-carbon fuels, Chem. Soc. Rev. 43 (2014) 631–675.

[3] X. Zhu, A. Yamamoto, S. Imai, A. Tanaka, H. Kominami, H. Yoshida, A silver-manganese dual co-catalyst for selective reduction of carbon dioxide into carbon monoxide over a potassium hexatitanate photocatalyst with water, Chem. Commun. 55 (2019) 13514–13517.

[4] K. Iizuka, T. Wato, Y. Miseki, K. Saito, A. Kudo, Photocatalytic reduction of carbon dioxide over Ag cocatalyst-loaded $ALa_4Ti_4O_{15}$ (A = Ca, Sr, and Ba) Using Water as a Reducing Reagent, J. Am.

Chem. Soc. 133 (2011) 20863–20868.

[5] N. Yamamoto, T. Yoshida, S. Yagi, Z. Like, T. Mizutani, S. Ogawa, H. Nameki, H. Yoshida, The inuence of the preparing method of a Ag/Ga_2O_3 catalyst on its activity for photocatalytic reduction of CO_2 with water, E-Journal Surf. Sci. Nanotechnol. 12 (2014) 263–268.

[6] M. Yamamoto, T. Yoshida, N. Yamamoto, T. Nomoto, Y. Yamamoto, S. Yagi, H. Yoshida, Photocatalytic reduction of CO_2 with water promoted by Ag clusters in Ag/Ga_2O_3 photocatalysts, J. Mater. Chem. A. 3 (2015) 16810–16816.

[7] Z. Wang, K. Teramura, S. Hosokawa, T. Tanaka, Photocatalytic conversion of CO_2 in water over Ag-modified La_2Ti2O_7, Appl. Catal. B Environ. 163 (2015) 241–247.

[8] A. Anzai, N. Fukuo, A. Yamamoto, H. Yoshida, Highly selective photocatalytic reduction of carbon dioxide with water over silver-loaded calcium titanate, Catal. Commun. 100 (2017) 134–138.

[9] H. Yoshida, L. Zhang, M. Sato, T. Morikawa, T. Kajino, T. Sekito, S. Matsumoto, H. Hirata, Calcium titanate photocatalyst prepared by a flux method for reduction of carbon dioxide with water, Catal. Today. 251 (2015) 132–139.

[10] Z. Chang, S. Huo, W. Zhang, J. Fang, H. Wang, The tunable and highly selective reduction products on Ag@Cu bimetallic catalysts toward CO_2 electrochemical reduction reaction, J. Phys. Chem. C. 121 (2017) 11368–11379.

[11] Q. Zhai, S. Xie, W. Fan, Q. Zhang, Y. Wang, W. Deng, Y. Wang, Photocatalytic conversion of carbon dioxide with water into methane: platinum and copper(I) oxide Co-catalysts with a core–shell structure, Angew. Chemie Int. Ed. 52 (2013) 5776–5779.

[12] R. Pang, K. Teramura, H. Tatsumi, H. Asakura, S. Hosokawa, T. Tanaka, Modification of Ga_2O_3 by an Ag-Cr core-shell cocatalyst enhances photocatalytic CO evolution for the conversion of CO_2 by H_2O, Chem. Commun. 54 (2018) 1053–1056.

[13] K. Maeda, A. Xiong, T. Yoshinaga, T. Ikeda, N. Sakamoto, T. Hisatomi, M. Takashima, D. Lu, M. Kanehara, T. Setoyama, T. Teranishi, K. Domen, Photocatalytic overall water splitting promoted by two different cocatalysts for hydrogen and oxygen evolution under visible light, Angew. Chemie

Int. Ed. 49 (2010) 4096–4099.

[14] Z. Jiang, D. Ding, L. Wang, Y. Zhang, L. Zan, Interfacial effects of MnO_x-loaded TiO_2 with exposed {001} facets and its catalytic activity for the photoreduction of CO_2, Catal. Sci. Technol. 7 (2017) 3065–3072.

[15] W. Tu, W. Guo, J. Hu, H. He, H. Li, Z. Li, W. Luo, Y. Zhou, Z. Zou, State-of-the-art advancements of crystal facet-exposed photocatalysts beyond TiO_2: Design and dependent performance for solar energy conversion and environment applications, Mater. Today. 33 (2020) 75–86.

[16] K. Wenderich, G. Mul, Methods, mechanism, and applications of photodeposition in photocatalysis: A Review, Chem. Rev. 116 (2016) 14587–14619.

[17] K. Teramura, Z. Wang, S. Hosokawa, Y. Sakata, T. Tanaka, A doping technique that suppresses undesirable H_2 evolution derived from overall water splitting in the highly selective photocatalytic conversion of CO_2 in and by water, Chem. – A Eur. J. 20 (2014) 9906–9909.

[18] S. Xie, Y. Wang, Q. Zhang, W. Deng, Y. Wang, $SrNb_2O_6$ nanoplates as efficient photocatalysts for the preferential reduction of CO_2 in the presence of H_2O, Chem. Commun. 51 (2015) 3430–3433.

[19] X. Zhu, A. Yamamoto, S. Imai, A. Tanaka, H. Kominami, H. Yoshida, Facet-selective deposition of a silver–manganese dual cocatalyst on potassium hexatitanate photocatalyst for highly selective reduction of carbon dioxide by water, Appl. Catal. B Environ. 274 (2020) 119085.

[20] X. Zhu, A. Anzai, A. Yamamoto, H. Yoshida, Silver-loaded sodium titanate photocatalysts for selective reduction of carbon dioxide to carbon monoxide with water, Appl. Catal. B Environ. 243 (2019) 47–56.

[21] T. Takata, J. Jiang, Y. Sakata, M. Nakabayashi, N. Shibata, V. Nandal, K. Seki, T. Hisatomi, K. Domen, Photocatalytic water splitting with a quantum efficiency of almost unity, Nature. 581 (2020) 411–414.

[22] Y.-F. Li, Z.-P. Liu, L. Liu, W. Gao, Mechanism and activity of photocatalytic oxygen evolution on titania anatase in aqueous surroundings, J. Am. Chem. Soc. 132 (2010) 13008–13015.

[23] Z. Fang, D.A. Dixon, Computational study of H_2 and O_2 production from water splitting by small

$(MO_2)_n$ clusters (M = Ti, Zr, Hf), J. Phys. Chem. A. 117 (2013) 3539–3555.

[24] H. Muraki, T. Saji, M. Fujihira, S. Aoyagui, Photocatalytic oxidation of water to hydrogen peroxide by irradiation of aqueous suspensions of TiO_2, J. Electroanal. Chem. Interfacial Electrochem. 169 (1984) 319–323.

[25] T. Ishii, A. Anzai, A. Yamamoto, H. Yoshida, Calcium zirconate photocatalyst and silver cocatalyst for reduction of carbon dioxide with water, Appl. Catal. B Environ. 277 (2020) 119192.

[26] M.S. Burke, S. Zou, L.J. Enman, J.E. Kellon, C.A. Gabor, E. Pledger, S.W. Boettcher, Revised oxygen evolution reaction activity trends for first-row transition-metal (Oxy)hydroxides in Alkaline Media, J. Phys. Chem. Lett. 6 (2015) 3737–3742.

[27] F. Meng, J. Li, S.K. Cushing, J. Bright, M. Zhi, J.D. Rowley, Z. Hong, A. Manivannan, A.D. Bristow, N. Wu, Photocatalytic water oxidation by hematite/reduced graphene oxide composites, ACS Catal. 3 (2013) 746–751.

[28] Q. Zhang, Z. Li, S. Wang, R. Li, X. Zhang, Z. Liang, H. Han, S. Liao, C. Li, Effect of redox cocatalysts location on photocatalytic overall water splitting over cubic $NaTaO_3$ semiconductor crystals exposed with equivalent facets, ACS Catal. 6 (2016) 2182–2191.